Organic & Biomolecular Chemistry

ROYAL SOCIETY OF CHEMISTRY

PAPER

View Article Online
View Journal | View Issue

Open Access Article. Published on 07 August 2023. Downloaded on 7/22/2025 8:26:15 PM.
This article is licensed under a Creative Commons Attribution-NonCommercial 3.0 Unported Licence.

Check for updates

Cite this: *Org. Biomol. Chem.*, 2023, **21**, 7005

Design, synthesis and structure–activity relationship studies on erianin analogues as pyruvate carboxylase inhibitors in hepatocellular carcinoma cells†

Hailong Shi,‡[a,b,c] Jinlian Yang,‡[a,b,c] Zeen Qiao,‡[a,b] Lingyu Li,[a,b] Gang Liu,[a,b] Qi Dai,[c] Li Xu,[c] Wei Jiao,[a] Guolin Zhang,[a] Fei Wang,[a] Xiaoxia Lu*[a,c] and Xiaofeng Ma*[a]

Received 12th July 2023,
Accepted 7th August 2023

DOI: 10.1039/d3ob01114c

rsc.li/obc

A series of novel erianin analogues were designed and synthesized based on the bioisosterism principle by altering the two aromatic rings of erianin, the substituents on the rings and the linker between them. The analogues were evaluated as pyruvate carboxylase (PC) inhibitors in hepatocellular carcinoma cells. It was found that compounds **35** and **36**, where fluorine replaces a hydroxyl group, exhibited higher activity than erianin (IC_{50} value of 17.30 nM) in liver cancer cells with IC_{50} values of 15.15 nM and 10.05 nM, respectively. Additionally, at a concentration of 10 nM, compounds **35** and **36** inhibited PC with inhibitory rates of 39.10% and 40.15%, respectively, exhibiting nearly identical inhibitory activity to erianin (inhibitory rate of 40.07%). Additionally, a computer simulation docking study demonstrated the basis for better interactions between the receptors and ligands. The fluorine atom of **35** can not only form hydrogen bonds with Lys-1043 (NH···F, 2.04 Å), but also form fluorine bonds with the carbonyl groups of Lys-1043 (3.67 Å) and Glu-1046 (3.70 Å), due to the different orientations of the halogens on the B ring warhead. Conversely, the chlorine atom of **34** can only form alkyl hydrophobic interactions with the alkane chain in Lys-1043. Fluorinated compounds **35** and **36** also show better chemical stability and higher log *P* (clog *P* = 3.89 for **35** and **36**) values than that of erianin (clog *P* = 3.07), and may be used as candidate compounds for further drug development.

1. Introduction

Accounting for 90% of liver cancers,[1] hepatocellular carcinoma (HCC) is the major histological subtype of liver cancer and the third most common cause of cancer-related mortality worldwide.[2] Liver transplantation is currently the most common treatment for liver cancer,[3] whilst high rates of tumour recurrence and metastasis are the main reason for the poor prognosis of hepatocellular carcinoma.[4] Moreover, more than 70% of patients with advanced stage HCC are not candidates for transplantation,[5] either due to tumour mutation burden (TMB) or poor liver function.[6] Ultimately, for most patients with advanced liver cancer, available treatments are unsatisfactory because: (i) few drugs that improve patient survival exist;[7] (ii) there are high incidences of treatment-related adverse events;[8] and (iii) mutated target proteins cause drug resistance, *etc.*[9] Therefore, to change the treatment landscape of HCC management at all stages, it is now highly desirable to develop novel diagnosis and treatment methods, including new diagnostic techniques, targeted drugs, immunotherapies, and combination therapies.[10]

Pyruvate carboxylase (PC) is a regulatory metabolic enzyme found mainly in the mitochondria that replenishes intermediates of the tricarboxylic acid cycle (TCA) and catalyses the first committed step of gluconeogenesis.[11] PC has been found to be overexpressed in multiple types of tumours,[12] and may also be overproduced in hepatocellular carcinoma. Targeting pyruvate carboxylase to inhibit the activity of excessively expressed PC in tumour cells is a potential target for the treatment of liver cancer *via* regulation of metabolic reprogramming. Over the past few decades, more than 20 PC inhibitors have been reported. However, most of these inhibitors have been used as molecular probes to elucidate various aspects of the structure and function of PC.[13] ZY-444 was the first reported anticancer

[a]*Natural Product Research Center, Chengdu Institute of Biology, Chinese Academy of Sciences, Chengdu, 610041, P. R. China. E-mail: maxf@cib.ac.cn, luxx@cib.ac.cn*
[b]*University of Chinese Academy of Sciences Institution Chinese Academy of Sciences Beijing, 100049, P. R. China*
[c]*NMPA Key Laboratory for Quality Monitoring and Evaluation of Traditional Chinese Medicine (Chinese Materia Medica), P. R. China*

† Electronic supplementary information (ESI) available. See DOI: https://doi.org/10.1039/d3ob01114c

‡ These authors contributed equally.

Open Access Article. Published on 07 August 2023. Downloaded on 7/22/2025 8:26:15 PM.
This article is licensed under a Creative Commons Attribution-NonCommercial 3.0 Unported Licence.

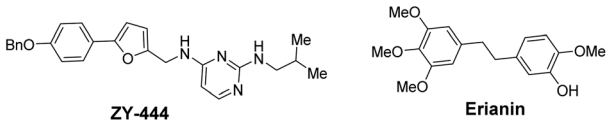

Fig. 1 PC inhibitors: ZY-444 and erianin.

molecule targeting PC (Fig. 1) and is a potent and selective PC inhibitor with an IC_{50} value of about 1 μM that suppresses breast cancer cell viability by 90% at 5 μM.[14] Despite its excellent potential in the treatment of breast cancer, no other case studies on the utilization of this inhibitor in clinical trials have been reported. Equally, no other anticancer treatments that utilize the inhibition of PC enzymes in other human cancers have been disclosed.

Erianin is a well-known natural product with a 1,2-diphenylethane scaffold that comes from the orchid plants *E. carinata*,[15] and has been reported as a highly efficient molecule against a variety of cancers, including hepatocellular carcinoma.[16] Recently, Wang and co-workers found that erianin inhibits PC with an IC_{50} value of 5 nM, regulates PC-mediated metabolic reprogramming to induce oxidative stress and inhibit glycolysis, activates the adenylate-activated protein kinase (AMPK) signalling pathway, and, ultimately, causes tumour cell apoptosis and inhibits tumour metastasis.[17] However, the lack of structure–activity relationship studies, its short half-life[18] and low bioavailability[19] have limited further drug development of erianin. These shortcomings of erianin may be related to the phenol fragment in its structure which is easily oxidized. Meanwhile, natural product-based drug development frequently uses the principle of bioisosterism to slightly alter the structure of natural products in order to enhance their affinity for the target while maintaining their biological activity. Herein, we disclose a structure–activity relationship study (SAR) of erianin to enhance its anticancer activity based on bioisosterism principles where the two aromatic rings of erianin, their ring substituents and the linker between them are changed (Fig. 2). 47 compounds were synthesized with different types of hydrophobic tail, various types and lengths of linkers, and divergent types of hydrogen bond donor (or acceptor) moieties. Biological activity against hepatocellular carcinoma cell lines was also investigated systematically. It was found that, of the 47 synthesized compounds, two exhibited better chemical stability and higher log*P* and enhanced activity in liver cancer cells by simply replacing easily the oxidized phenolic hydroxyl group with a fluorine atom.

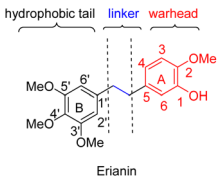

Fig. 2 The proposed molecular pharmacophore model of erianin.

2. Results and discussion

2.1 Design

Based on the analysis of the results of a preliminary activity study of the 14 natural analogues of erianin and a molecular simulation docking by Wang,[17] some preliminary conclusion could be drawn: (i) the three methoxy groups on the B ring are indispensable to the maintenance of biological activity; (ii) the linear-linker between the two aromatic rings is necessary because the formation of a 6 membered ring with either the A ring or B ring resulted in a decrease in the activity; (iii) the introduction of strong hydrophilic fragment such as a sugar on the A ring or the B ring is unfavourable for biological activity; and (iv) interchanging the positions of the hydroxyl and methoxy groups on the A ring also seemed to greatly affect the activity. According to these conclusions, we hypothesized that the obvious cytotoxicity of erianin might be because its structure has a hydrophobic tail and a warhead moiety (hydrogen-bond donor or acceptor) linked by an appropriate linker (Fig. 2). Based on the principle of bioisosterism, we designed a series of compounds in which the hydroxyl group of the A ring was replaced with its classical electron–isostere halogen, the A and B rings were replaced with similar aromatic rings, and the linkers between the benzene rings were replaced with isosteres. Using these strategies, 47 erianin analogues were synthesized and then subjected to bioactive assessment.

2.2 Chemistry

The compounds tested during this study were synthesized through seven different, though complementary routes (Schemes 1–7). Compounds **1–4** were synthesized according to reported literature procedures (Schemes 1 and 2).[20,21] For the synthesis of **5**,[22] **14**[23] and **15** (Scheme 3), the corresponding aryl bromides, were treated with *n*-butyl lithium, the obtained aryl lithium were then captured with Weinreb amides to produce intermediates **S3-1** to **S3-3**. The products **5**, **14** and **15** can be smoothly obtained *via* the catalytic hydrogenation of **S3-1** to **S3-3**.

Compound **6** was obtained by using aryl amine **S4-1** as the starting material, which was obtained according to a reported literature procedure.[24] Thus, **S4-1** was treated with sodium hydride (NaH) and methyl iodide (MeI), and under these con-

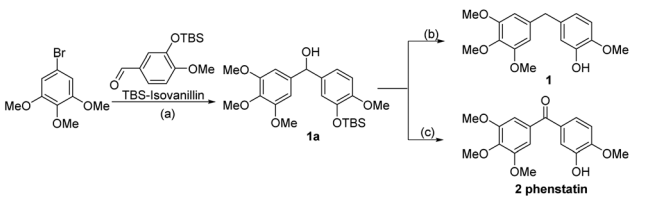

Scheme 1 Synthetic route for compounds **1** and **2**. Reagents and conditions: (a) *n*-BuLi, then TBS-Isovanillin, THF, −78 °C to 25 °C, 0.5 h, 86.2%; (C) (i): PDC, DCM, 25 °C, 1 h, 90.1%; (ii): TBAF, THF, 25 °C, 3 h, 89.7%; (b) (i): Et_3SiH, TFA, DCM, 0 °C to 25 °C, 2.5 h, 75.4%; (ii): TBAF, THF. 25 °C, 3 h, 98.5%.

Open Access Article. Published on 07 August 2023. Downloaded on 7/22/2025 8:26:15 PM.
This article is licensed under a Creative Commons Attribution-NonCommercial 3.0 Unported Licence.

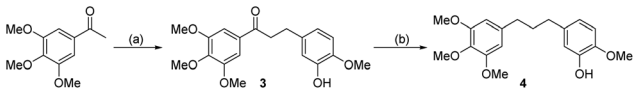

Scheme 2 Synthetic route for compounds **3** and **4**. Reagents and conditions: (a) (i): Isovanillin, Pyrrolidine, AcOH, THF, 65 °C, 8 h, 82%; (ii): Pd/C, H_2, diphenyl sulfide, MeOH, 25 °C, 2 h, 86.5 %; (b) Pd/C, H_2, AcOH, 25 °C,12 h, 91.4%.

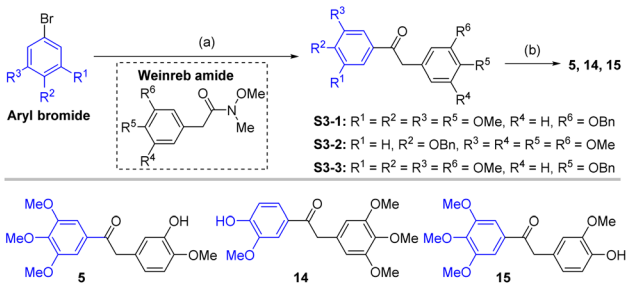

Scheme 3 Synthetic route for compounds **5**, **14** and **15**. Reagents and conditions: (a) aryl bromide, *n*-BuLi, THF, −78 °C, 0.5 h; then Weinreb amide, −78 °C, 1 h; (b) Pd/C, H_2, MeOH, 25 °C, 4 h, 85.7–92.3%.

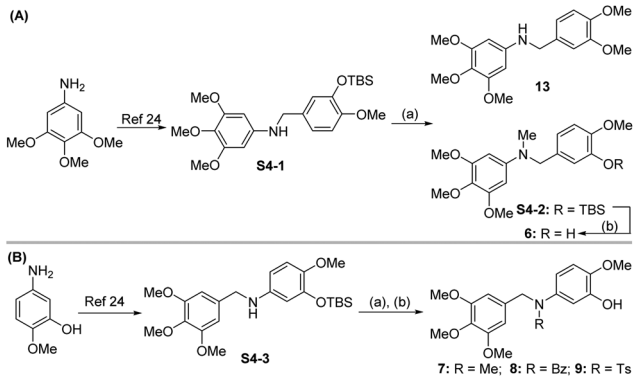

Scheme 4 Synthetic route for compounds **6–9** and **13**. Reagents and conditions: (a) MeI or BzCl or TsCl, NaH, THF, 0 °C,1.5 h, 58.6–99.1%; (b) TBAF, THF, 25 °C, 3 h, 82.7–92.1%.

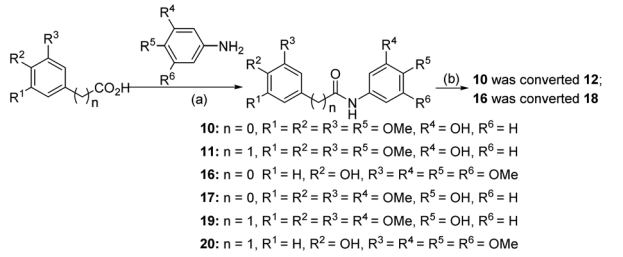

Scheme 5 Synthetic route for compounds **10–12** and **16–20**. Reagents and conditions: (a) carboxylic acids, anilines, HATU, DMF, 0 °C to 25 °C, 2 h, 73.5–83.2%; (b) Lawesson's reagent, toluene, reflux, 0.5 h, 66.3–78.2%.

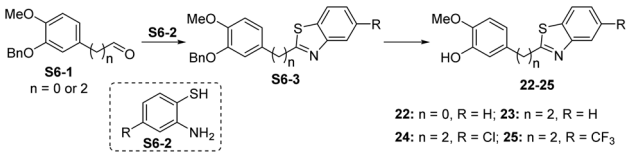

Scheme 6 Synthetic route for compounds **22–25**. Reagents and conditions: (a) **S6-1**, **S6-2**, TsOH–H_2O, Na_2SO_4, DMF, N_2, 120 °C, 10–30 min, 21–39%; (b) con. HCl/AcOH (1 : 2), 80 °C, 10 min, 38–78%.

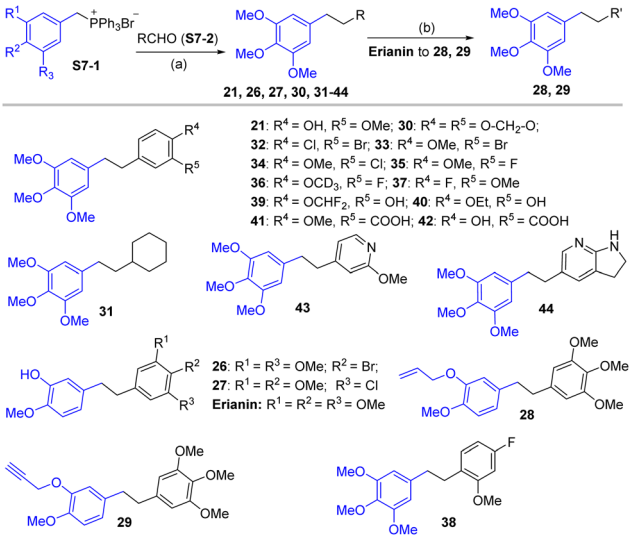

Scheme 7 Synthetic route for compounds **26–44**. Reagents and conditions: (a) (i) **S7-1**, **S7-2**, NaH, THF, 0 °C–25 °C, 12 h; (ii) Pd/C, H_2, MeOH, 0 °C–25 °C, 4 h; (b) allyl bromide or 3-bromopropyne, K_2CO_3, THF, 25 °C, 4 h.

ditions, besides the desired methylation product **S4-2**, a byproduct (**13**) was also formed *via* the concurrent deprotection-methylation of the *tert*-butyldimethylsilyl (TBS) protected phenol hydroxyl group. The TBS protecting group in **S4-2** can be smoothly removed in the presence of tetrabutylammonium fluoride (TBAF) to deliver **6** (Scheme 4A). This procedure can also be used to synthesize **7**,[24] **8** and **9**, in which the free amine was protected by methyl (Me), benzoyl (Bz) and toluenesulfonyl (Ts) groups (Scheme 4B). Compounds **10**, **11**, **16**, **17**, **19**, and **20** were obtained directly by condensation of the corresponding carboxylic acids with amines in the presence of HATU in DMF, while the thioamide compounds **12** and **18** were produced by treatment of **10**[24] and **16** respectively with Lawesson's reagent (Scheme 5). The synthesis of **22–25** involves the condensation and oxidative aromatization between an aryl substituted aldehyde and a substituted 2-aminophenylthiophenol (**S6-1**) to give intermediate **S6-3**, which was followed by debenzylation in the presence of concentrated hydrochloric acid (Scheme 6). The preparations of erianin,[24] **21**,[25] **26**, **27** and **30–44** were achieved through a Wittig reaction between triphenyl (substituted benzyl)-phosphonium bromide and the corresponding aldehydes to obtained alkenes, which was then followed by catalytic hydrogenation. Compounds **28**

Open Access Article. Published on 07 August 2023. Downloaded on 7/22/2025 8:26:15 PM.
This article is licensed under a Creative Commons Attribution-NonCommercial 3.0 Unported Licence.

and **29** were obtained by direct alkylation of the hydroxyl group of erianin (Scheme 7).

For those substrates such as **45–47**, in which the aldehydes are not readily available, the 3,4,5-trimethoxybromobenzene derivative **S8-1** was coupled with an aryl bromide **S8-2** under Sonogashira cross-coupling conditions to generate **S8-3**, which was then hydrogenated under catalytic hydrogenation conditions (Scheme 8).

2.3 Structure–activity relationships

2.3.1 Optimization of the linkers between the diphenyl rings. We first investigated the effect of the length and type of carbon chain in erianin on its *anti*-human-hepatocellular-carcinoma activity (Table 1). Compared with the parent molecule erianin, shortening (such as in compound **1**) or increasing (such as in compound **4**) the length of the chain between the two phenyl rings could lead to a decreasing in the activity. Changing the linker to a ketone generated compounds phenstatin **2**, **3** and **5**. Of these compounds, phenstatin (**2**) with only a carbonyl group linking the two phenyl rings showed the strongest activity, whereas the bioactivity of compounds **3** and **5** was reduced to varying degrees. The carbon chain was then changed to an N-substituted methylene amino (–$NRCH_2$–) linker. It was found that, among compounds **6–9** and **13**, **6** has slightly better activity than the other four. Compared with **6**, compound **7**, in which the order of the linker between the A and B ring was interchanged, showed sharply decreased bioactivity. When the substituent on the N-atom was changed from a methyl to a benzoyl group in **8** and a *p*-toluenesulfonyl group in **9**, the bioactivity was also reduced. At a concentration of 50 nM, the inhibition rate of compounds **10–12**, linked with an amide or thioamide, on the HCCLM3 cell line did not exceed 10%. This situation didn't change even when the concentration was increased to 200 nM, and this may indicate that the rigid amides and thioamides as linkers were detrimental to the improvement of the biological activity of the compounds. To compare, we also synthesized substrates by exchanging the substitution position of the hydroxyl and methoxy groups on the A ring of erianin (**14–21**) and investigated the influence of this change on the bioactivity. It was found that the bioactivity of compounds **14–21** decreased

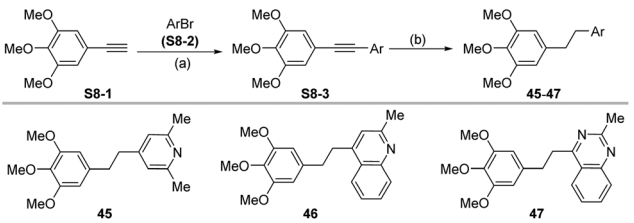

Scheme 8 Synthetic route for compounds **45–47**. Reagents and conditions: (a) **S8-1**, **S8-2**, Pd $(PPh_3)_4$ (6 mol%), CuI (6 mol%), XantPhos (6 mol%), Et_3N, 1,4-dioxane, reflux,14 h; (b) Pd/C, H_2, MeOH, 25 °C, 12 h. 34.3–62.5%.

Table 1 Investigation of the linkers between the two aromatic groups

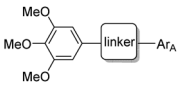

No.	Linkers	Ar_A	HCCLM3 % (50 nM)[a]	HCCLM3 % (200 nM)[b]	No.	Linkers	Ar_A	HCCLM3 % (50 nM)[a]	HCCLM3 % (200 nM)[b]
1	–CH_2–		65.17 ± 0.72	74.29 ± 2.37	13	–$NHCH_2$–		25.90 ± 2.22	23.85 ± 2.91
2	–CO–		81.14 ± 0.63	94.18 ± 0.56	14	–CH_2CO–		36.64 ± 1.64	31.62 ± 4.32
3	–$CO(CH_2)_2$–		39.62 ± 0.47	76.55 ± 2.66	15	–$COCH_2$–		23.02 ± 2.53	28.01 ± 1.83
4	–$(CH_3)_3$–		54.15 ± 3.25	76.91 ± 1.88	16	–NHCO–		29.66 ± 2.25	43.83 ± 1.50
5	–$COCH_2$–		3.51 ± 0.16	41.02 ± 3.62	17	–CONH–		23.02 ± 6.70	28.01 ± 1.03
6	-NCH_2- (Me)		64.48 ± 1.23	75.96 ± 2.81	18	–CSNH–		0.60 ± 0.27	0.62 ± 0.11
7	-CH_3N- (Me)		30.83 ± 3.26	44.96 ± 6.94	19	–CH_2CONH–		9.44 ± 3.17	7.32 ± 2.41
8	-CH_3N- (Bz)		36.28 ± 2.21	46.00 ± 8.35	20	–$NHCOCH_2$–		ND	NT
9	-CH_2N- (Ts)		25.77 ± 2.46	41.39 ± 5.16	21	–$(CH_2)_2$–		0.45 ± 0.16	3.17 ± 0.56
10	–CONH–		8.54 ± 1.71	20.16 ± 3.70	Erianin			67.59 ± 2.26	78.86 ± 1.35
11	–CH_2CONH		5.32 ± 1.45	8.17 ± 8.01					
12	–CSNH–		4.27 ± 0.18	4.83 ± 2.17					

[a] % (50 nM) values of the erianin analogues on cell growth inhibition in HCCLM3 at a concentration of 50 nM. [b] % (200 nM) values of the erianin analogues on cell growth inhibition in HCCLM3 at a concentration of 200 nM. Data are mean values ± SD of $n = 3$. ND = NO detection, NT = NO test.

Open Access Article. Published on 07 August 2023. Downloaded on 7/22/2025 8:26:15 PM.
This article is licensed under a Creative Commons Attribution-NonCommercial 3.0 Unported Licence.

significantly, and for compounds **18**, **20** and **21**, no bioactivity was detected at all.

Based on the preliminary screening of the activity of more than 20 erianin analogues with different linkers, we may conclude the following: the linker between the two substituted phenyl rings requires a flexible carbon chain (such as in compounds **1**, **4** and erianin) or a flexible C–N chain (such as in compound **6**) to maintain the bioactivity; the length of the linker should be two methylene units or a single methylene unit with an extra tertiary amine attached to Ar_A; elongating or shortening the length of the linker was detrimental to bioactivity; and increasing the molecular rigidity, such as with carbonyl (compounds **2**, **3** and **5**), amide (compounds **10**, **11**) and thioamide (compound **12**) groups, or increasing the steric hindrance of the substituent on the N-atoms (compounds **8**, **9**) of the linkers reduces the bioactivities. Furthermore, it was found that the hydroxyl group at the 1-position of the A ring was essential for the bioactivity. Therefore, we then fixed the linker as two methylene units and the A ring as 1-hydroxyl-2-methoxyl phenyl and proceeded to investigate the effect that changing the substituents on the B ring has on the bioactivities.

2.3.2 Optimization of the Ar_B ring. Compounds **22–25** are erianin derivatives in which the B ring of erianin was replaced by different substituted benzothiazole rings. The inhibition rates for most of these molecules at 50 nM remained about 40% (except **25**, 15.2%), while at 200 nM, the inhibition rate did not increase significantly (Table 2). When one of the three methoxy groups in the B ring was replaced by a halogen, such as 4-bromo-substituted analogue **26** and 3-chloro-substituted analogue **27**, the bioactivities almost completely disappeared. This was similar to our previous results,[17] as it was found that the bioactivity of 4-demethylerianin (**4-DMER**) and 5,4′-dimethoxybibenzyl-3,3′-diol (**DMBZD**) (Fig. 3a), which have free hydroxyl groups on the B ring, was much weaker than that of erianin. Comparing **4-DMER** and **DMBZD** with compounds **22–27**, there is not much difference in molecular size, but the clog *P* values are very different (Fig. 3b). From these results, it seems that possessing an appropriate log *P* is an important factor for the bioactivity of an analogue. To further explain the difference in bioactivity between erianin and compound **23**, which have similar log *P* values, we extracted fragments of Ar_B (the other parts of these compounds were exactly the same) and calculated their clog *P* values (Fig. 3c). It was found that the clog *P* values of the B ring fragments (Ar_B**22–27**) of **22–27** were significantly larger than the B ring value of erianin. Moreover, although the clog *P* values of Ar_B-**4-DMER** and Ar_B-**DMBZD** were similar to that of erianin, the activity of these two compounds was seriously lost due to the hydroxyl group on the ring. In view of this, we believe that the B ring should not have hydrogen bond donors such as hydroxyl groups directly linked to the aromatic ring and should have a suitable clog *P* value to balance the hydrophobicity of the B ring region of the compound. At this point, we have identified the effect that the B ring composition and the linkers between the two aromatic fragments have on the bioactivity. Next, we conducted a systematic study on the effect that the A ring has on the bioactivities.

2.3.3 Optimization of the Ar_A ring. During the investigation of the influence of the linkers on the bioactivities, we speculated that the 1-hydroxyl group of the A ring was crucial. To further clarify this, we synthesized compounds **28–30** in which the hydroxyl group was protected by allyl, propargyl or methylene groups. In addition, we also replaced the A ring with cyclo-

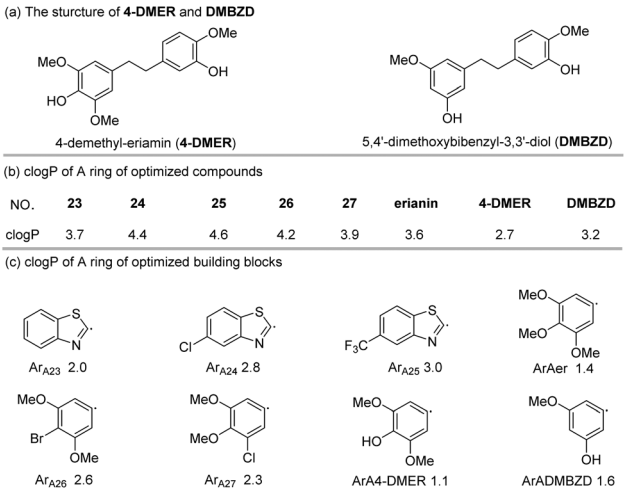

Fig. 3 clog *P* values of the B rings of optimized compounds and building blocks.

Table 2 Optimization of the Ar_B ring

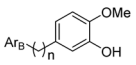

No.	Ar_B	*n*	HCCLM3 % (50 nM)[a]	HCCLM3 % (200 nM)[b]
22		0	33.60 ± 3.53	25.20 ± 4.00
23		2	35.39 ± 5.91	44.07 ± 4.55
24	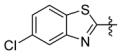	2	36.55 ± 4.94	43.52 ± 2.28
25	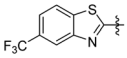	2	15.20 ± 2.41	12.05 ± 0.82
26		2	ND	NT
27	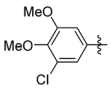	2	9.61 ± 3.10	9.86 ± 3.72
Erianin	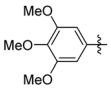	2	67.59 ± 2.26	78.86 ± 1.35

[a] % (50 nM) values of the erianin analogues on cell growth inhibition in HCCLM3 at a concentration of 50 nM. [b] % (200 nM) values of the erianin analogues on cell growth inhibition in HCCLM3 at a concentration of 200 nM. Data are mean values SD of $n = 3$. ND = NO detection, NT = NO test.

Open Access Article. Published on 07 August 2023. Downloaded on 7/22/2025 8:26:15 PM.
This article is licensed under a Creative Commons Attribution-NonCommercial 3.0 Unported Licence.

Table 3 Optimization of the Ar_A ring

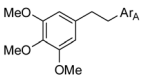

No.	Ar_A	HCCLM3 % (50 nM)[a]	HCCLM3 % (200 nM)[b]	No.	Ar_A	HCCLM3 % (50 nM)[a]	HCCLM3 % (200 nM)[b]	No.	Ar_A	HCCLM3 % (50 nM)[a]	HCCLM3 % (200 nM)[b]
28	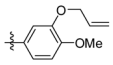	7.10 ± 2.85	30.23 ± 1.98	35	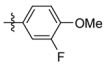	66.61 ± 5.45	64.23 ± 5.68	42		17.71 ± 0.72	20.79 ± 1.23
29	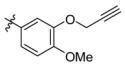	7.47 ± 0.70	32.00 ± 1.61	36	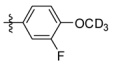	57.39 ± 3.70	60.56 ± 4.45	43		10.27 ± 1.49	13.52 ± 2.22
30		2.04 ± 2.32	3.24 ± 1.62	37	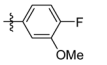	16.53 ± 0.63	6.64 ± 1.37	44		ND	NT
31		7.17 ± 3.01	8.14 ± 6.65	38		ND	NT	45		5.47 ± 1.19	18.62 ± 3.46
32		1.04 ± 0.43	16.23 ± 1.54	39	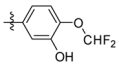	9.48 ± 4.36	20.59 ± 6.43	46		3.15 ± 1.12	7.89 ± 1.96
33	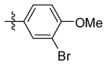	42.14 ± 1.62	19.60 ± 3.19	40	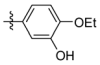	5.64 ± 1.10	10.33 ± 2.54	47		13.61 ± 5.29	11.60 ± 2.11
34	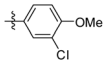	40.49 ± 2.81	72.32 ± 3.57	41	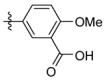	0.84 ± 0.36	3.44 ± 1.17	Erianin		67.59 ± 2.26	78.86 ± 1.35

[a] % (50 nM) values of the erianin analogues on cell growth inhibition in HCCLM3 at a concentration of 50 nM. [b] % (200 nM) values of the erianin analogues on cell growth inhibition in HCCLM3 at a concentration of 200 nM. Data are mean values SD of $n = 3$. ND = NO detection, NT = NO test.

hexyl (**31**) and 3-Br–4-Cl phenyl (compound **32**) moieties and tested the bioactivities of these compounds (Table 3). The results showed that the bioactivities are dramatically decreased, which further confirmed our hypothesis. However, compounds **33–35**, in which the 1-hydroxyl group of the A ring was replaced by bromine, chlorine and fluorine, respectively, showed very good bioactivity. Of these compounds, the 1-fluoro analogue had similar bioactivity to erianin; this could be because the fluorine and hydroxyl groups are bioisosteres. We also synthesized the deuterated derivative (**36**) of **35** and it was found that compound **36** has better bioactivity. Compounds **37** and **38**, in which the positions of the fluorine and methoxy groups are interchanged, showed much worse bioactivity. The bioactivity of compounds **32**, **39** and **40** were also greatly reduced, indicating that the 2-methoxy group is also indispensable. Compared with erianin, the introduction of carboxylic acids to the A ring (such as in compounds **41** and **42**), or the replacement of the A ring with nitrogen-containing aromatic rings (such as in compounds **43–47**), significantly reduce the bioactivity as well.

2.3.4 Inhibition of pyruvate carboxylase (PC). Compounds with good inhibition rates, **1–4**, **6**, and **34–36**, were then used in assays of the half inhibitory concentration (IC_{50}) of the HCCLM3 cell line (Fig. 4 and Fig. S1†) and the inhibition of pyruvate carboxylase (Fig. 5). All the tested compounds showed

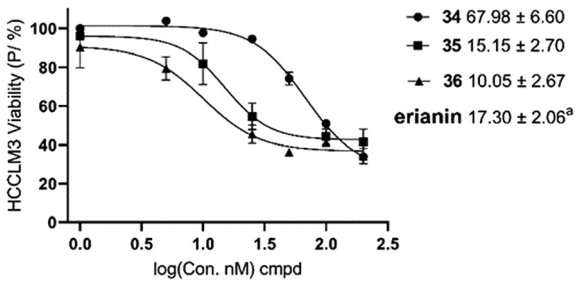

Fig. 4 IC_{50} values of the erianin analogues on cell growth inhibition in HCCLM3. [a]IC_{50} value of erianin.[17] Data are mean values ± SE of $n = 3$.

cytotoxicity against the HCCLM3 cells, and of these, the IC_{50} values of compounds **1**, **6**, **35**, and **36** were less than 30 nM. These compounds (especially **34–36**) also had a significant inhibitory effect on pyruvate carboxylase activity, even at a concentration of 10 nM. The PC inhibition results show that, compared to compounds **1–3** and **6** which have been reported as anticancer agents (**1**,[20] **2**[20] and **6**[24] as tubulin inhibitors; and **3** as a nuclear factor-κB (NF-κB) inhibitor[21]), erianin and compounds **34–36** have better selectivity against pyruvate carboxylase. The cytotoxic activity of compound **35** was equivalent to erianin, while **36** was stronger than erianin. However, deute-

Open Access Article. Published on 07 August 2023. Downloaded on 7/22/2025 8:26:15 PM.
This article is licensed under a Creative Commons Attribution-NonCommercial 3.0 Unported Licence.

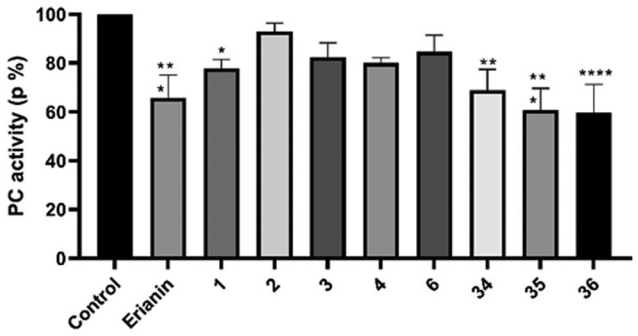

Fig. 5 Inhibition of pyruvate carboxylase (PC) at a concentration of 10 nM. Data are mean values ± SD of n = 3.

rated compound **36**, which has better cell-level bioactivity, exhibited almost identical PC inhibition activity to that of **35**. This may be related to the fact that the deuterated methyl group has no obvious isotope effect on PC.

2.4 Molecular docking

The possible binding modes of the synthesized erianin analogues were studied by molecular docking calculations using the X-ray structure of human pyruvate carboxylase (PC, PDB ID: 3GB3). The results of the simulated molecular docking showed that the Libdock-scores of compounds **34**, **35** and erianin were 84.47, 93.39 and 80.09, respectively. This was consistent with the order of inhibitory potency of these compounds on PC at 10 nM. Comparison of the binding modes of compound **35** with that of compound **34** and erianin (Fig. 6 and Fig. SI2–4†) showed an inversion of its binding orientation in the active site of 3GB3. The binding sites and the dominant conformation of **34** and **35** were at the same active binding site of PC. However, due to the different orientations of the halogens on the A ring warhead, the fluorine atom of **35** can not only form hydrogen bonds with Lys-1043 (NH···F, 2.04 Å), but also form fluorine bonds with the carbonyl groups of Lys-1043 (3.67 Å) and Glu-1046 (3.70 Å). In the optimum binding conformation of compound **34**, the orientation of the chlorine atom was opposite to that of the fluorine atom in compound **35**, and this chlorine atom can only form alkyl hydrophobic interactions with the alkane chain of Lys-1043. The binding region of erianin was also similar to that of compounds **34** and **35**. However, the optimal binding site (Fig. SI2–4†) and conformation were different (Fig. 6, C(3D)). The hydroxyl group in the warhead of erianin can form hydrogen bonds with Gln-1073 (2.98 Å) as a hydrogen bond donor and Gln-1075 (3.07 Å) as a hydrogen bond acceptor.

3. Conclusions

In conclusion, we present a systemic structure–activity relationship study on erianin, which has previously been identified as a pyruvate carboxylase (PC)-targeting *anti*-hepatocellular carcinoma agent. Our studies showed that a strongly lipophilic two-atom bridge ($-CH_2CH_2-$, $-NMeCH_2-$) linker could be optimal distance between the two rings. An essential component for strong anticancer activity of the whole molecule was the retention of amphiprotic A-ring fragments with low clog P values as a hydrophobic tail. When the B ring had a higher or lower clog P value, but a hydroxyl group substituted directly on the benzene, the activity of the molecules was greatly reduced. With respect to the A ring, the 1-hydroxyl group was found to be an important pharmacophore, and it could be replaced by halogen groups (Br, Cl, F). Additionally, compounds **35** and **36**, where the hydroxyl groups were replaced by fluorine atoms, had the same or even better activity as erianin. The optimal substituents on the oxygen at the 2-position of the A ring were –Me and $-CD_3$, while difluoromethyl and ethyl groups on the 2-position oxygen of erianin lead to a dramatic decrease in the activity.

Fluorinated compounds **35** and **36** had similar activity to erianin but had higher liposolubility (clog P 35 = clog P 36 = 3.89, @ChemDraw) and more chemical stability than erianin. These compounds may be used as candidates for the treatment or diagnosis of central nervous system (CNS) tumours and may even penetrate the brain through the blood–brain barrier. Furthermore, the research presented here would be valuable for the development of more anticancer candidates with similar core structures, higher activity and oral bio-

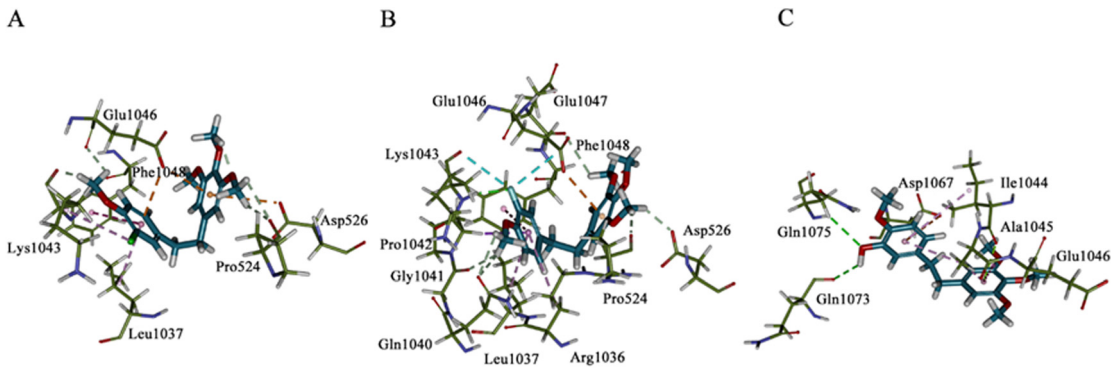

Fig. 6 Binding conformations of **34**, **35** and erianin with human pyruvate carboxylase (PDB ID: 3BG3). Panel A–C(3D): binding modes of compound **34** (panel A), **35** (panel B), and erianin (panel C) in the active site of 3BG3.

Open Access Article. Published on 07 August 2023. Downloaded on 7/22/2025 8:26:15 PM.
This article is licensed under a Creative Commons Attribution-NonCommercial 3.0 Unported Licence.

availability. This research may even further improve the selectivity of PC inhibition and the molecules presented may serve as a chemical probe to determine whether PC can be used as a druggable target. Research is ongoing to further refine the selectivity for the PC inhibition and to identify a chemical probe for the dissection of PC-dependent tumour energy metabolism pathways and will be reported in due course.

4. Experimental section

4.1 Chemistry and synthesis

The synthesis and characterization of compounds **1–7**, **10**, **14**, **21**, **39** and **40** had already been reported in previous studies.[21–27] The compounds **8**, **9**, **11–13**, **15–20**, **22–34**, **36–38** and **41–47** were synthesized according to the route in Schemes 3–8. The structures of all compounds were confirmed from the analytical data obtained from ^{1}H NMR and ^{13}C NMR spectroscopies, and mass spectrometry. All reagents were purchased from commercial suppliers (Energy Chemical, Bide Pharma) and were of the highest commercial quality and used without further purification. All reactions were performed with magnetic stirring and were followed using thin layer chromatography (TLC) on silica gel 60 F254 precoated plates (0.25 mm, Yantai Jiangyou silica gel Development Co., Ltd) and the pure compound was visualized under UV light. Purification of the reaction products was carried out using flash column chromatography (FCC) using ultra-pure silica gel (200–300 mesh) purchased from Yantai Jiangyou silica gel Development Co., Ltd, unless otherwise stated. Nuclear magnetic resonance (NMR) spectra were recorded on Bruker Avance spectrometers (^{1}H NMR at 400 MHz or 600 MHz, ^{13}C NMR at 101 MHz or 150 MHz). High-resolution mass spectra (HRMS) were obtained using MicrOTOF-Q II mass spectrometer in ESI mode.

General synthetic procedure for 8, 9, and 13. To a cooled solution (ice bath) of monosubstituted aniline (**6a** or **7a**, 1 eq.) in dry DMF, was added sodium hydride (1.2 eq.) under an argon atmosphere. The reaction mixture was stirred for about 15 min at the same temperature, and to it was added respectively methyl iodide (1.2 eq.)/benzoyl chloride (1.15 eq.)/*p*-toluene sulfonyl chloride (1.15 eq.), and the resulting mixture was stirred for another 0.5–1 h. The reaction mixture was poured into ice-cooled water and was extracted with ethyl acetate (3 × 20 mL). The combined organic layers were dried over sodium sulphate (Na_2SO_4) and evaporated under reduced pressure. The crude product was then dissolved in THF (5 mL), and a solution of tetrabutylammonium fluoride in THF (TBAF, 2.5 eq.) was added at 25 °C. The mixture was then stirred for 1 h. The reaction was quenched with water, extracted with ethyl acetate (3 × 20 mL). The combined organic layers were dried over sodium sulphate (Na_2SO_4) and evaporated under reduced pressure. The crude product was purified *via* silica gel column chromatography (ethyl acetate : hexane = 1 : 5) to yield the corresponding product.

*N-(3,4-Dimethoxybenzyl)-3,4,5-trimethoxyaniline (**13**).* 170 mg, 44% yield. ^{1}H NMR (400 MHz, $CDCl_3$) δ 6.93 (t, 2H), 6.85 (d, J = 8.64 Hz, 1H), 5.90 (s, 2H), 4.23 (s, 2H), 3.88 (d, J = 2.04 Hz, 6H), 3.80 (s, 6H), 3.77 (s, 3H); ^{13}C NMR (101 MHz, $CDCl_3$) δ 153.95, 149.16, 148.31, 145.08, 131.78, 130.20, 119.84, 111.18, 110.88, 90.45, 61.11, 55.96, 55.93, 55.89, 48.82; HRMS-ESI + (m/z): calcd for $C_{18}H_{23}NO_5$ [M + H]$^+$: 334.1654, found: 334.1664.

*N-(3-Hydroxy-4-methoxyphenyl)-N-(3,4,5-trimethoxybenzyl) benzamide (**8**).* 387.7 mg, 92% yield. ^{1}H NMR (400 MHz, $CDCl_3$) δ 7.35 (d, J = 7.04 Hz, 2H), 7.19–7.21 (m, 3H), 6.64 (d, J = 2.36 Hz, 1H), 6.54 (t, J = 4.6 Hz, 3H), 6.31 (d, J = 8.32 Hz, 1H), 5.80 (s, 1H), 4.98 (s, 2H), 3.83 (s, 3H), 3.78 (s, 6H), 3.77 (s, 3H); ^{13}C NMR (101 MHz, $CDCl_3$) δ 170.57, 153.13, 145.82, 145.37, 137.24, 136.86, 136.16, 133.36, 133.35, 129.54, 128.50, 127.74, 120.06, 113.96, 110.25, 105.62, 60.84, 56.09, 55.89, 54.09; HRMS-ESI + (m/z): calcd for $C_{24}H_{25}NO_6$ [M + H]$^+$: 424.1760, found: 424.1769.

*N-(3-Hydroxy-4-methoxyphenyl)-4-methyl-N-(3,4,5-trimethoxybenzyl) benzenesulfonamide (**9**).* 217.6 mg, 83% yield. ^{1}H NMR (400 MHz, $CDCl_3$) δ 7.58 (d, J = 8.24 Hz, 2H), 7.27 (d, J = 8.04 Hz, 2H), 6.68 (d, J = 8.6 Hz, 1H), 6.57 (dd, J = 2.48, 8.56 Hz, 1H), 6.50 (d, J = 2.48 Hz, 1H), 6.43 (s, 2H), 5.57 (s, 1H), 4.59 (s, 2H), 3.82 (s, 3H), 3.78 (s, 3H), 3.77 (s, 6H), 2.44 (s, 3H); ^{13}C NMR (101 MHz, $CDCl_3$) δ 153.06, 146.17, 145.45, 143.90, 137.26, 135.71, 132.18, 131.71, 129.51, 127.77, 121.74, 114.53, 110.23, 105.46, 60.79, 56.06, 55.90, 55.14; HRMS-ESI + (m/z): calcd for $C_{24}H_{27}NO_7S$ [M + Na]$^+$: 496.1406, found: 496.1420.

General synthetic procedure for 11, 16, 17, 19 and 20. Under a nitrogen atmosphere, substituted anilines (1.0 eq.) and substituted carboxylic acids (1.1 eq.) were mixed in DMF. HATU (1.2 eq.) was added at 0 °C. The resulting mixture was stirred for 2–3 h. Water was then added to quench the reaction, and the mixture was extracted with ethyl acetate (3 × 5 mL). The combined organic layers were dried over sodium sulphate (Na_2SO_4) and evaporated under reduced pressure, and the crude product was crystallized in methanol to obtain the product.

*N-(3-Hydroxy-4-methoxyphenyl)-2-(3,4,5-trimethoxyphenyl)-acetamide (**11**).* 384.6 mg, 83% yield. ^{1}H NMR (400 MHz, DMSO-d_6) δ 9.87 (s, 1H), 8.72 (s, 1H), 7.28 (d, J = 2.16 Hz, 1H), 6.93 (dd, J = 6.93, 8.48 Hz, 1H), 6.67 (d, J = 8.48 Hz, 1H), 6.64 (s, 2H), 3.77 (s, 6H), 3.72 (s, 3H), 3.63 (s, 3H), 3.50 (s, 2H), 3.35 (s, 1H); ^{13}C NMR (101 MHz, DMSO-d_6) δ 168.79, 153.11, 147.63, 142.89, 136.67, 132.22, 131.87, 115.63, 112.17, 106.94, 105.15, 60.43, 56.28, 55.91, 44.01; HRMS-ESI + (m/z): calcd for $C_{18}H_{21}NO_6$ [M + H]$^+$: 348.1447, found: 348.1449.

*4-Hydroxy-3-methoxy-N-(3,4,5-trimethoxyphenyl) benzamide (**16**).* 395.5 mg, 79.2% yield. ^{1}H NMR (400 MHz, $CDCl_3$) δ 7.90 (s, 1H), 7.52 (d, J = 1.52 Hz, 1H), 7.34 (dd, J = 1.64, 8.24 Hz, 1H), 6.96 (s, 2H), 6.95 (d, J = 8.28 Hz, 1H), 6.07 (s, 1H), 3.93 (s, 3H), 3.84 (s, 6H), 3.83 (s, 3H); ^{13}C NMR (101 MHz, $CDCl_3$) δ 165.29, 153.36, 149.17, 146.89, 134.77, 134.24, 126.89, 119.72, 114.02, 110.52, 97.89, 61.00, 56.09; HRMS-ESI + (m/z): calcd for $C_{17}H_{19}NO_6$ [M + H]$^+$: 334.1290, found: 334.1290.

*N-(4-Hydroxy-3-methoxyphenyl)-3,4,5-trimethoxybenzamide (**17**).* 367.3 mg, 73.5% yield. ^{1}H NMR (400 MHz, DMSO-d_6) δ 9.92 (s, 1H), 8.81 (s, 1H), 7.39 (d, J = 2.12 Hz, 1H), 7.27 (s, 2H),

Open Access Article. Published on 07 August 2023. Downloaded on 7/22/2025 8:26:15 PM. This article is licensed under a Creative Commons Attribution-NonCommercial 3.0 Unported Licence.

7.12 (dd, J = 2.00, 8.48 Hz, 1H), 6.76 (d, J = 8.52 Hz, 1H), 3.87 (s, 6H), 3.77 (s, 3H), 3.73 (s, 3H); ^{13}C NMR (101 MHz, DMSO-d$_6$) δ 164.42, 152.31, 145.49, 141.71, 140.17, 129.75, 129.37, 113.16, 112.06, 103.83, 103.43, 59.94, 55.36, 55.00; HRMS-ESI + (m/z): calcd for $C_{17}H_{19}NO_6$ [M + H]$^+$: 334.1290, found: 334.1290.

*N-(4-Hydroxy-3-methoxyphenyl)-2-(3,4,5-trimethoxyphenyl) acetamide (**19**).*. 384.6 mg, 83.2% yield. ^{1}H NMR (400 MHz, DMSO-d$_6$) δ 9.87 (s, 1H), 8.72 (s, 1H), 7.28 (d, J = 2.16 Hz, 1H), 6.93 (dd, J = 6.93, 8.48 Hz, 1H), 6.67 (d, J = 8.48 Hz, 1H), 6.64 (s, 2H), 3.77 (s, 6H), 3.72 (s, 3H), 3.63 (s, 3H), 3.50 (s, 2H), 3.35 (s, 1H); ^{13}C NMR (101 MHz, DMSO-d$_6$) δ 168.79, 153.11, 147.63, 142.89, 136.67, 132.22, 131.87, 115.63, 112.17, 106.94, 105.15, 60.43, 56.28, 55.91, 44.01; HRMS-ESI + (m/z): calcd for $C_{18}H_{21}NO_6$ [M + H]$^+$: 348.1447, found: 348.1445.

*2-(4-Hydroxy-3-methoxyphenyl)-N-(3,4,5-trimethoxyphenyl) acetamide (**20**).* 204.6 mg, 68.2% yield. ^{1}H NMR (400 MHz, DMSO-d$_6$) δ 9.84 (s, 1H), 9.02 (s, 1H), 7.16 (d, J = 2.36 Hz, 1H), 6.93 (dd, J = 2.36, 8.64 Hz, 1H), 6.80 (d, J = 8.72 Hz, 1H), 6.64 (s, 2H), 3.76 (s, 6H), 3.71 (s, 3H), 3.63 (s, 3H), 3.50 (s, 2H), 3.35 (s, 1H); ^{13}C NMR (101 MHz, DMSO-d$_6$) δ 168.86, 153.12, 146.85, 144.21, 136.66, 133.32, 132.23, 112.93, 110.38, 108.22, 106.88, 60.43, 56.33, 56.27, 44.00; HRMS-ESI + (m/z): calcd for $C_{18}H_{21}NO_6$ [M + H]$^+$: 348.1368, found: 348.1446.

General synthetic procedure for 12 and 18. To a suspension of **10** or **17** in toluene was added Lawesson's reagent (0.58 eq.) at 25 °C, the resulting mixture was refluxed for 0.5 h, cooled and then the mixture was concentrated under reduced pressure to obtain a residue, which was purified directly by column chromatography (DCM : MeOH = 50 : 1–15 : 1) to yield a pale yellow solid.

*N-(3-Hydroxy-4-methoxyphenyl)-3,4,5-trimethoxybenzothioamide (**12**).* 66.3 mg, 66% yield. ^{1}H NMR (400 MHz, DMSO-d$_6$) δ 11.41 (s, 1H), 9.16 (s, 1H), 7.46 (d, J = 2.08 Hz, 1H), 7.18 (s, 2H), 7.15 (d, J = 2.12 Hz, 1H), 6.81 (d, J = 8.44 Hz, 1H), 3.85 (s, 6H), 3.76 (s, 3H), 3.72 (s, 3H); ^{13}C NMR (101 MHz, DMSO-d$_6$) δ 195.84, 152.50, 147.39, 145.33, 140.06, 138.16, 132.31, 117.54, 115.21, 109.76, 105.66, 60.58, 56.46, 56.16. HRMS-ESI + (m/z): calcd for $C_{17}H_{19}NO_5S$ [M + H]$^+$: 350.1062, found: 350.1064.

*N-(4-Hydroxy-3-methoxyphenyl)-3,4,5-trimethoxybenzothioamide (**18**).* 78.2 mg, 78% yield. ^{1}H NMR (400 MHz, DMSO-d$_6$) δ 11.33 (s, 1H), 9.70 (s, 1H), 7.50 (s, 1H), 7.40 (d, J = 8.16 Hz, 1H), 7.26 (s, 2H), 6.83 (d, J = 8.48 Hz, 1H), 3.84 (s, 3H), 3.76 (s, 6H), 3.68 (s, 3H); ^{13}C NMR (101 MHz, DMSO-d$_6$) δ 196.41, 152.83, 150.23, 147.09, 136.59, 135.78, 133.97, 121.72, 114.92, 112.54, 102.59, 60.58, 56.39, 56.14; HRMS-ESI + (m/z): calcd for $C_{17}H_{19}NO_5S$ [M + H]$^+$: 350.1062, found: 350.1064.

Synthetic procedure for compound 15. Bromo-3,4,5-trimethoxybenzene (200.0 mg, 0.81 mmol) was dissolved in anhydrous THF (5 mL) and the solution was then cooled to −78 °C under a nitrogen atmosphere. A solution of n-BuLi in THF (1.6 M, 0.61 mL, 1.2 eq.) was then added slowly, and the resulting mixture was stirred at the same temperature for 0.5 h. To this mixture, a solution of 2-(4-(benzyloxy)-3-methoxyphenyl)-N-methoxy-N-methyl acetamide (268.5 mg, 0.89 mmol) in THF was then added, and the reaction mixture was stirred for another 0.5 h. The reaction was then quenched by the addition of saturated ammonium chloride solution, and the mixture was extracted with ethyl acetate (3 × 20 mL). The combined organic layers were dried over sodium sulphate (Na_2SO_4) and evaporated under reduced pressure. Then, the residue was subjected to silica gel column chromatography (petroleum ether : ethyl acetate = 3 : 1) to obtain a white solid **S3-3** (289 mg, 85% yield). The obtained ketone **S3-3** (100.0 mg, 0.24 mmol) was dissolved in THF (4 mL), 10% palladium on carbon (25.2 mg) was added to the solution. The reaction vessel was evacuated and backfilled with hydrogen (H_2) five times. The mixture was stirred at room temperature for 12 h and then filtered through Celite give a filtrate. This filtrate was evaporated to oil, which was purified by chromatography on silica gel (ethyl acetate : hexane = 1 : 3) to give **15** (63.0 mg, 80% yield). ^{1}H NMR (400 MHz, CDCl$_3$) δ 7.29 (s, 2H), 6.89 (d, J = 8.52 Hz, 1H), 6.80 (dd, J = 1.84, 5.28 Hz, 1H), 4.19 (s, 2H), 3.93 (s, 3H), 3.91 (s, 6H), 3.88 (s, 3H); ^{13}C NMR (101 MHz, CDCl$_3$) δ 196.82, 153.03, 146.75, 144.70, 142.66, 131.70, 126.54, 122.15, 114.56, 111.61, 106.32, 60.93, 56.27, 55.90, 45.30. HRMS-ESI + (m/z): calcd for $C_{17}H_{19}NO_5S$ [M + H]$^+$: 350.1062, found: 350.1064.

General synthetic procedure for 22 and 25. A mixture of aldehydes (0.74 mmol, 1 eq.), 2-aminobenzenethiols (0.89 mmol, 1.2 eq.), TsOH·$H_2$0 (1.11 eq.), and anhydrous Na_2SO_4 (1.11 eq.) in DMF was heated at 120 °C for 1–4 h, the reaction mixture was then cooled to room temperature and concentrated under reduced pressure, the resulting residue was then purified by column chromatography (ethyl acetate : hexane = 1 : 5) to yield a pale yellow slurry. To this slurry was added a pre-prepared mixture of concentrated hydrochloric acid/acetic acid (v/v 2 : 1, 2 mL) and the resulting mixture was heated at 80 °C for 5–15 min. The reaction solution was cooled to room temperature and water was then added, and the acid neutralized with 1 N sodium hydroxide solution. The mixture was extracted with ethyl acetate (3 × 20 mL). The combined organic layers were then dried over sodium sulphate (Na_2SO_4) and evaporated under reduced pressure. The obtained residue was purified by chromatography on silica gel (10% ethyl acetate : hexane = 1 : 10) to give the products.

*5-(Benzo[d]thiazol-2-yl)-2-methoxyphenol (**22**).* 38 mg, 8% yield over two steps. ^{1}H NMR (400 MHz, CDCl$_3$) δ 8.04 (d, J = 8.16 Hz, 1H), 7.87 (d, J = 7.96 Hz, 1H), 7.63–7.67 (m, 2H), 7.45–7.49 (m, 1H), 7.33–7.38 (m, 1H), 6.94 (d, J = 8.28 Hz, 1H), 5.73 (s, 1H), 3.97 (s, 3H); ^{13}C NMR (101 MHz, CDCl$_3$) δ 167.83, 154.18, 149.02, 145.97, 134.98, 127.22, 126.21, 124.86, 122.93, 121.51, 120.06, 113.73, 110.72, 56.09; HRMS-ESI + (m/z): calcd for $C_{14}H_{11}NO_2S$ [M + H]$^+$: 258.0589, found: 258.0588.

*5-(2-(Benzo[d]thiazol-2-yl)ethyl)-2-methoxyphenol (**23**).* 65 mg, 14% yield over two steps. ^{1}H NMR (400 MHz, CDCl$_3$) δ 7.96 (s, 1H), 7.72 (d, J = 7.80 Hz, 1H), 7.33 (dd, J = 1.36, 8.44 Hz, 1H), 6.83 (s, 1H), 6.77 (d, J = 8.20 Hz, 1H), 6.71 (d, J = 8.12 Hz, 1H), 5.70 (s, 1H), 3.85 (s, 3H), 3.38 (t, J = 8.24 Hz, 2H), 3.10 (t, J = 8.20 Hz, 2H); ^{13}C NMR (101 MHz, CDCl$_3$) δ 173.13, 154.05, 145.67, 145.28, 133.41, 133.23, 131.96, 125.23, 122.49, 122.20, 119.83, 114.68, 110.77, 55.98, 36.14, 34.77; HRMS-ESI + (m/z): calcd for $C_{16}H_{15}NO_2S$ [M + H]$^+$: 286.0902, found: 286.0897.

Open Access Article. Published on 07 August 2023. Downloaded on 7/22/2025 8:26:15 PM.
This article is licensed under a Creative Commons Attribution-NonCommercial 3.0 Unported Licence.

*5-(2-(5-Chlorobenzo[d]thiazol-2-yl)ethyl)-2-methoxyphenol (**24**).* 62 mg, 24% yield over two steps. ^{1}H NMR (400 MHz, $CDCl_3$) δ 7.95 (d, J = 1.92 Hz, 1H), 7.73 (d, J = 8.52 Hz, 1H), 7.33 (dd, J = 1.96, 8.52 Hz, 1H), 6.83 (d, J = 1.92 Hz, 1H), 6.76 (d, J = 8.16 Hz, 1H), 6.71 (dd, J = 1.92, 8.20 Hz, 1H), 5.73 (s, 1H), 3.85 (s, 3H), 3.38 (t, J = 7.48 Hz, 2H), 3.11 (t, J = 8.28 Hz, 2H); ^{13}C NMR (101 MHz, $CDCl_3$) δ 173.13, 154.05, 145.67, 145.28, 133.41, 133.23, 131.96, 125.23, 122.49, 122.20, 119.83, 114.68, 110.77, 55.98, 36.14, 34.77; HRMS-ESI + (m/z): calcd for $C_{16}H_{14}ClNO_2S$ [M + H]$^+$: 320.0512, found: 320.0514.

*2-Methoxy-5-(2-(5-(trifluoromethyl)benzo[d]thiazol-2-yl)ethyl) phenol (**25**).* 78 mg, 23% yield over two steps.^{1}H NMR (400 MHz, DMSO-d$_6$) δ 8.84 (s, 1H), 8.31 (d, 2H), 7.72 (d, J = 8.36 Hz, 1H), 6.79 (d, J = 8.16 Hz, 1H), 6.71 (s, 1H), 6.64 (d, J = 8.08 Hz, 1H), 3.72 (s, 3H), 3.43 (t, J = 15.48 Hz, 2H), 3.02 (t, J = 7.48 Hz, 2H); ^{13}C NMR (100 MHz, DMSO-d$_6$) δ 174.63, 152.73, 146.81, 146.61, 139.44, 132.97, 127.58, 127.26, 126.18, 124.02, 123.47, 121.35, 121.32, 119.41, 119.37, 116.25, 112.65, 56.05, 35.72, 34.22; HRMS-ESI + (m/z): calcd for $C_{17}H_{14}F_3NO_2S$ [M + H]$^+$: 354.0775, found: 354.0779.

General synthetic procedure for 26–44. To a stirred solution of **S7-1**[28] (0.383 mmol, 1 eq.) in THF (8 mL) was added sodium hydride (1.5 eq.) at 0 °C. After stirring at the same temperature for 10 min, **S7-2** (0.95 eq.) was added to the reaction mixture at 0 °C. The ice bath was removed, and the mixture was stirred for another 12 h. The reaction mixture was neutralized with NH_4Cl and then the aqueous layer was extracted with ethyl acetate (4 × 20 mL), the combined organic layer was dried over Na_2SO_4 and concentrated under vacuum to give the compound as a yellow solid which was directly used as the raw material in the next reaction.

To a stirred solution of the products of the previous reaction (0.383 mmol, 1 eq.) in methanol (5 mL) was added Pd/C (0.1 eq.) at room temperature. The reaction vessel was evacuated and back-filled with hydrogen (H_2) five times. The reaction mixture was stirred in a hydrogen atmosphere at rt for 4 h. After completion of the reaction, the reaction mixture was filtered, and the filtrate was evaporated under vacuum to afford the crude product which was purified by column chromatography on silica gel with ethyl acetate/hexane (1/5) to provide **26–44**.

*5-(4-Bromo-3,5-dimethoxyphenethyl)-2-methoxyphenol (**26**).* 110 mg, 78% yield over two steps. ^{1}H NMR (400 MHz, $CDCl_3$) δ 6.82 (d, J = 2.0 Hz, 1H), 6.78 (d, J = 8.2 Hz, 1H), 6.63 (dd, J = 8.1, 2.0 Hz, 1H), 6.38 (s, 2H), 5.58 (s, 1H), 3.89 (s, 3H), 3.87 (s, 6H), 2.86 (t, J = 3.8 Hz, 4H); ^{13}C NMR (101 MHz, $CDCl_3$) δ 156.76, 145.50, 144.91, 142.58, 134.60, 119.91, 114.63, 110.54, 105.13, 98.07, 56.39, 56.03, 38.43, 37.07, 29.72; HRMS-ESI + (m/z): calcd for $C_{17}H_{18}BrO_4$ [M + Na]$^+$: 389.0364; found: 389.0363.

*5-(3-Chloro-4,5-dimethoxyphenethyl)-2-methoxyphenol (**27**).* 96 mg, 78% yield over two steps. ^{1}H NMR (400 MHz, $CDCl_3$) δ 6.82 (d, J = 1.9 Hz, 1H), 6.80 (d, J = 4.6 Hz, 1H), 6.78–6.75 (m, 1H), 6.70–6.63 (m, 2H), 5.57 (s, 1H), 3.89 (d, J = 3.3 Hz, 6H), 3.87 (s, 3H), 2.84 (s, 4H); ^{13}C NMR (101 MHz, $CDCl_3$) δ 148.67, 147.17, 145.43, 144.79, 135.17, 134.49, 120.21, 119.83, 114.67, 111.84, 111.14, 110.53, 56.02, 55.92, 55.79, 37.61, 37.50; HRMS-ESI + (m/z): calcd for $C_{17}H_{19}ClO_4$ [M + H]$^+$: 323.1090; found: 323.1092.

*5-(3-(Allyloxy)-4-methoxyphenethyl)-1,2,3-trimethoxybenzene (**28**).* 126 mg, 92% yield over three steps. ^{1}H NMR (400 MHz, $CDCl_3$) δ 6.83 (d, J = 8.1 Hz, 1H), 6.75 (dd, J = 8.1, 1.8 Hz, 1H), 6.70 (d, J = 1.8 Hz, 1H), 6.38 (s, 2H), 6.15–6.03 (m, 1H), 5.41 (dd, J = 17.2, 1.5 Hz, 1H), 5.30 (dd, J = 10.5, 1.2 Hz, 1H), 4.59 (d, J = 5.4 Hz, 2H), 3.88 (s, 3H), 3.85 (d, J = 2.2 Hz, 9H), 2.85 (s, 4H); ^{13}C NMR (101 MHz, $CDCl_3$) δ 153.02, 147.75, 137.50, 136.14, 134.13, 133.41, 120.82, 117.90, 114.14, 111.63, 105.42, 69.89, 60.89, 56.05, 38.48, 37.46; HRMS-ESI + (m/z): calcd for $C_{21}H_{26}O_5$ [M + Na]$^+$: 381.1677; found: 381.1678.

*1,2,3-Trimethoxy-5-(4-methoxy-3-(prop-2-yn-1-yloxy)phenethyl) benzene (**29**).* 127 mg, 93% yield over three steps. ^{1}H NMR (400 MHz, $CDCl_3$) δ 6.87 (d, J = 1.7 Hz, 1H), 6.84 (d, J = 8.2 Hz, 1H), 6.82–6.78 (m, 1H), 6.37 (s, 2H), 4.75 (d, J = 2.3 Hz, 2H), 3.88 (s, 3H), 3.84 (d, J = 2.9 Hz, 9H), 2.92–2.84 (m, 4H), 2.52 (t, J = 2.3 Hz, 1H); ^{13}C NMR (101 MHz, $CDCl_3$) δ 153.01, 147.99, 146.50, 137.40, 136.12, 134.10, 121.93, 115.10, 111.73, 105.43, 78.67, 75.72, 60.88, 56.79, 56.06, 56.00, 38.42, 37.37; HRMS-ESI + (m/z): calcd for $C_{21}H_{24}O_5$ [M + Na]$^+$: 381.1678; found: 381.1678.

*5-(2-Cyclohexylethyl)-1,2,3-trimethoxybenzene (**31**).* 77 mg, 72% yield over two steps. ^{1}H NMR (400 MHz, $CDCl_3$) δ 6.41 (s, 2H), 3.88 (s, 6H), 3.85 (s, 3H), 2.58 (dd, J = 9.5, 6.9 Hz, 2H), 1.79 (d, J = 13.6 Hz, 2H), 1.73–1.67 (m, 2H), 1.55–1.49 (m, 2H), 1.34–1.26 (m, 3H), 1.23 (d, J = 10.1 Hz, 2H), 1.02–0.92 (m, 2H); ^{13}C NMR (101 MHz, $CDCl_3$) δ 153.02, 139.09, 135.84, 105.13, 60.87, 56.04, 39.50, 37.49, 33.78, 33.35, 26.70, 26.37; HRMS-ESI + (m/z): calcd for $C_{17}H_{26}O_3$ [M + H]$^+$: 279.1960; found: 279.1956.

*5-(3-Bromo-4-chlorophenethyl)-1,2,3-trimethoxybenzene (**32**).* 106 mg, 72% yield over two steps. ^{1}H NMR (400 MHz, $CDCl_3$) δ 7.37 (d, J = 8.2 Hz, 1H), 7.15–7.02 (m, 2H), 6.36 (s, 2H), 3.85 (d, J = 1.0 Hz, 6H), 3.84 (s, 3H), 2.91–2.83 (m, 4H); ^{13}C NMR (101 MHz, $CDCl_3$) δ 153.08, 141.90, 140.00, 136.57, 133.75, 131.87, 130.00, 128.75, 128.41, 105.38, 60.91, 56.06, 38.19, 37.29, 36.98; HRMS-ESI + (m/z): calcd for $C_{18}H_{19}BrClO_3$ [M + H]$^+$: 385.0206; found: 385.0206.

*5-(3-Bromo-4-methoxyphenethyl)-1,2,3-trimethoxybenzene (**33**).* 118 mg, 81% yield over two steps. ^{1}H NMR (400 MHz, $CDCl_3$) δ 7.39 (d, J = 1.7 Hz, 1H), 7.10–7.03 (m, 1H), 6.83 (d, J = 8.3 Hz, 1H), 6.37 (s, 2H), 3.89 (s, 3H), 3.85 (d, J = 2.3 Hz, 9H), 2.84 (s, 4H); ^{13}C NMR (101 MHz, $CDCl_3$) δ 154.16, 153.08, 137.10, 136.26, 135.27, 133.27, 128.46, 111.83, 111.36, 105.43, 60.89, 56.30, 56.07, 38.36, 36.73; HRMS-ESI + (m/z): calcd for $C_{18}H_{21}BrO_4$ [M + Na]$^+$: 403.0521; found: 403.0520.

*5-(3-Chloro-4-methoxyphenethyl)-1,2,3-trimethoxybenzene (**34**).* 98 mg, 76% yield over two steps. ^{1}H NMR (400 MHz, $CDCl_3$) δ 7.22 (d, J = 2.0 Hz, 1H), 7.02 (dd, J = 8.3, 2.1 Hz, 1H), 6.86 (d, J = 8.4 Hz, 1H), 6.37 (s, 2H), 3.91 (s, 3H), 3.85 (d, J = 1.8 Hz, 9H), 2.85 (s, 4H); ^{13}C NMR (101 MHz, $CDCl_3$) δ 153.08, 137.11, 136.24, 134.79, 130.22, 127.68, 122.08, 111.98, 105.40, 60.90, 56.21, 56.07, 38.33, 36.81, 29.72; HRMS-ESI + (m/z): calcd for $C_{18}H_{19}F_3O_5$ [M + Na]$^+$: 359.1026; found: 359.1025.

*5-(3-Fluoro-4-methoxyphenethyl)-1,2,3-trimethoxybenzene (**35**).* 120 mg, 98% yield over two steps. ^{1}H NMR (400 MHz, $CDCl_3$) δ 6.97–6.93 (m, 1H), 6.88 (d, J = 6.9 Hz, 2H), 6.37 (s, 2H), 3.89 (s,

Open Access Article. Published on 07 August 2023. Downloaded on 7/22/2025 8:26:15 PM. This article is licensed under a Creative Commons Attribution-NonCommercial 3.0 Unported Licence.

3H), 3.85 (d, J = 1.2 Hz, 9H), 2.85 (s, 4H); ^{13}C NMR (101 MHz, $CDCl_3$) δ 153.08, 137.13, 136.25, 134.75, 124.00, 123.97, 116.22, 116.04, 113.36, 105.39, 60.89, 56.40, 56.07, 38.23, 36.95; HRMS-ESI + (m/z): calcd for $C_{18}H_{21}FO_4$ [M + Na]$^+$: 326.1368; found: 326.1367.

*5-(3-Fluoro-4-(methoxy-d$_3$) phenethyl-d$_3$)-1,2,3-trimethoxybenzene (**36**).* 109 mg, 88% yield over two steps. ^{1}H NMR (400 MHz, $CDCl_3$) δ 6.95 (d, J = 12.2 Hz, 1H), 6.92–6.84 (m, 2H), 6.38 (s, 2H), 3.85 (s, 9H), 2.85 (s, 4H); ^{13}C NMR (101 MHz, $CDCl_3$) δ 153.46, 153.07, 151.02, 137.14, 136.22, 134.68, 124.01, 123.97, 116.22, 116.04, 113.33, 105.36, 60.89, 56.06, 38.24, 36.95; HRMS-ESI + (m/z): calcd for $C_{18}H_{18}D_3FO_4$ [M + Na]$^+$: 346.1510; found: 346.1509.

*5-(4-Fluoro-3-methoxyphenethyl)-1,2,3-trimethoxybenzene (**37**).* 234 mg, 36% yield over two steps. ^{1}H NMR (400 MHz, DMSO-d$_6$) δ 7.08 (dd, J = 8.24, 11.68 Hz, 1H), 7.02 (dd, J = 1.76, 8.52 Hz, 1H), 6.77–6.81 (m, 1H), 6.54 (s, 2H), 3.81 (s, 3H), 3.74 (s, 6H), 3.62 (s, 3H), 2.77–2.87 (m, 4H); ^{13}C NMR (100 MHz, DMSO-d$_6$) δ 153.12, 149.23, 147.12, 138.84, 137.61, 136.07, 120.84, 115.88, 114.44, 106.10, 60.41, 56.27, 56.21, 38.0, 37.23; HRMS-ESI + (m/z): calcd for $C_{18}H_{21}FO_4$ [M + H]$^+$: 321.1502, found: 321.1508.

*5-(4-Fluoro-2-methoxyphenethyl)-1,2,3-trimethoxybenzene (**38**).* 271 mg, 42% yield over two steps. ^{1}H NMR (400 MHz, DMSO-d$_6$) δ 7.13 (t, J = 7.8 Hz, 1H), 6.84 (d, J = 11.44 Hz, 1H), 6.65–6.69 (m, 1H), 6.46 (s, 2H), 3.80 (s, 3H), 3.73 (s, 6H), 3.62 (s, 3H), 2.71–2.82 (m, 4H); ^{13}C NMR (101 MHz, DMSO-d$_6$) δ 160.90, 158.61, 153.09, 137.87, 136.85, 130.70, 125.78, 106.34, 105.94, 99.34, 60.39, 56.15, 36.16, 31.44; HRMS-ESI + (m/z): calcd for $C_{18}H_{21}FO_4$ [M + H]$^+$: 321.1502, found: 321.1501.

*2-Methoxy-5-(3,4,5-trimethoxyphenethyl) benzoic acid (**41**).* 94 mg, 71% yield over two steps. ^{1}H NMR (400 MHz, DMSO-d$_6$) δ 7.52 (s, 1H), 7.36 (d, J = 8.3 Hz, 1H), 7.03 (d, J = 8.5 Hz, 1H), 6.54 (s, 2H), 3.78 (s, 3H), 3.74 (s, 6H), 2.87–2.74 (m, 4H); ^{13}C NMR (101 MHz, DMSO-d$_6$) δ 168.04, 156.77, 153.09, 137.60, 136.05, 133.60, 133.19, 130.96, 121.69, 112.83, 106.14, 60.41, 56.23, 56.20, 39.97, 38.11, 36.42; HRMS-ESI + (m/z): calcd for $C_{19}H_{22}O_6$ [M + Na]$^+$: 369.1314; found: 369.1317.

*2-Hydroxyl-5-(3,4,5-trimethoxyphenethyl) benzoic acid (**42**).* 67 mg, 53% yield over two steps. ^{1}H NMR (400 MHz, $CDCl_3$) δ 10.28 (s, 1H), 7.24 (d, J = 2.04 Hz, 1H), 7.33 (dd, J = 2,16, 8.48 Hz, 1H), 6.95 (d, J = 8.48 Hz, 1H), 6.37 (s, 2H), 3.84 (s, 3H), 3.83 (s, 6H), 2.81–2.91 (m, 4H); ^{13}C NMR (101 MHz, $CDCl_3$) δ 174.49, 160.56, 153.10, 137.44, 137.01, 136.27, 132.69, 117.70, 111.00, 105.52, 60. 90, 56.10, 38.28, 36.84; HRMS-ESI + (m/z): calcd for $C_{18}H_{20}O_6$ [M + Na]$^+$: 355.1158; found: 355.1166.

*2-Methoxy-5-(3,4,5-trimethoxyphenethyl) pyridine (**43**).* 99 mg, 85% yield over two steps. ^{1}H NMR (400 MHz, $CDCl_3$) δ 7.98 (d, J = 2.1 Hz, 1H), 7.38 (dd, J = 8.5, 2.4 Hz, 1H), 6.69 (d, J = 8.5 Hz, 1H), 6.37 (s, 2H), 3.94 (s, 3H), 3.85 (d, J = 2.0 Hz, 9H), 2.85 (s, 4H); ^{13}C NMR (101 MHz, $CDCl_3$) δ 162.78, 153.11, 146.14, 139.06, 136.84, 136.31, 129.37, 110.35, 105.44, 60.89, 56.07, 53.34, 38.16, 34.01; HRMS-ESI + (m/z): calcd for $C_{17}H_{21}NO_4$ [M + Na]$^+$: 326.1368; found: 326.1367.

*5-(3,4,5-Trimethoxyphenethyl)-2,3-dihydro-1H-pyrrolo[2,3-b] pyridine (**44**).* 55 mg, 46% yield over two steps. ^{1}H NMR (400 MHz, $CDCl_3$) δ 7.02 (s, 1H), 6.98 (s, 1H), 6.41 (s, 2H), 3.99 (s, 2H), 3.85 (d, J = 1.9 Hz, 9H), 3.08 (t, J = 8.7 Hz, 2H), 2.85 (s, 4H); ^{13}C NMR (101 MHz, $CDCl_3$) δ 153.04, 137.66, 136.12, 135.57, 127.31, 114.49, 105.33, 77.35, 76.72, 60.89, 56.06, 47.66, 38.75, 37.50, 28.50; HRMS-ESI + (m/z): calcd for $C_{18}H_{22}N_2O_3$ [M + Na]$^+$: 337.1528; found: 337.1527.

General synthetic procedure for 45–47. Aryl bromides (3.55 mmol, 1.2 eq.), trimethoxy phenylacetylene **S8-1**[29] (2.96 mmol, 1.0 eq.), cuprous iodide (0.18 mmol, 0.06 eq.), Xantphos (0.18 mmol, 0.06 eq.) were placed into a Schlenk tube (20.0 mL) with a magnetic stirrer bar. The reaction vessel was evacuated and backfilled with nitrogen three times, then 1,4-dioxane (10.0 mL) was added under a positive nitrogen pressure. Subsequently, tetra(triphenylphosphine) palladium (0.18 mmol) and triethylamine (8.88 mmol, 3.0 eq.) were added. The reaction was heated at 80 °C for 12 h. After cooling to room temperature, the suspension was filtered through a pad of Celite, and the filtrate was concentrated *in vacuo*. The residue was purified by silica gel column chromatography to afford the corresponding product.

To a stirred solution of the above obtained products (1,2-disubstituted acetylene, 0.66 mmol, 1.0 eq.) in THF (6 mL) was added Pd/C (0.3 eq.), and then the reaction vessel was evacuated and backfilled with hydrogen (H_2) five times. The mixture was stirred at room temperature for 12 h. After completion of the reaction, the reaction mixture was evaporated under vacuum to afford the crude product which was purified by column chromatography on silica gel (ethyl acetate : hexane = 1 : 3) to provide the product.

*2,6-Dimethyl-4-(3,4,5-trimethoxyphenethyl) pyridine (**45**).* 114 mg, 34.3% yield over two steps. ^{1}H NMR (400 MHz, $CDCl_3$) δ 6.79 (s, 2H), 6.36 (s, 2H), 3.83 (s, 3H), 3.83 (s, 6H), 3.82 (s, 3H), 2.83 (s, 4H), 2.49 (s, 6H); ^{13}C NMR (101 MHz, $CDCl_3$) δ 157.60, 153.14, 150.90, 136.81, 136.42, 120.48, 105.40, 60.86, 56.07, 37.14, 24.37; HRMS-ESI + (m/z): calcd for $C_{18}H_{23}NO_3$ [M + H]$^+$: 302.1756, found: 302.1760.

*2-Methyl-4-(3,4,5-trimethoxyphenethyl) quinoline (**46**).* 156 mg, 62.6% yield over two steps. ^{1}H NMR (400 MHz, $CDCl_3$) δ 8.03 (d, J = 8.36 Hz, 1H), 7.97 (d, J = 8.28 Hz, 1H), 7.68 (t, J = 7.52 Hz, 1H), 7.50 (t, J = 7.36 Hz, 1H), 7.09 (s, 1H), 6.36 (s, 2H), 3.84 (s, 3H), 3.81 (s, 6H), 3.33 (t, J = 6.36 Hz, 3H), 3.01 (t, J = 7.48 Hz, 2H), 2.70 (s, 3H); ^{13}C NMR (101 MHz, $CDCl_3$) δ 158.64, 153.23, 148.11, 147.23, 136.81, 136.78, 129.49, 129.09, 125.68, 125.54, 123.15, 121.83, 105.46, 60.90, 56.12, 36.67, 34.08, 25.31; HRMS-ESI + (m/z): calcd for $C_{21}H_{23}NO_3$ [M + H]$^+$: 338.1756, found: 338.1762.

*2-Methyl-4-(3,4,5-trimethoxyphenethyl) quinazoline (**47**).* 275 mg, 51.5% yield over two steps. ^{1}H NMR (400 MHz, $CDCl_3$) δ 8.03 (d, J = 8.16 Hz, 1H), 7.96 (d, J = 8.36 Hz, 1H), 7.81–7.86 (m, 1H), 6.46 (s, 2H), 3.82 (s, 3H), 3.81 (s, 6H), 3.52–3.56 (m, 2H), 3.14 (dd, J = 5.92, 8.36 Hz, 2H), 2.89 (s, 3H); ^{13}C NMR (101 MHz, $CDCl_3$) δ 170.26, 163.70, 153.23, 150.35, 136.87, 136.52, 133.53, 128.46, 126.60, 124.40, 121.48, 105.50, 60.87, 56.10, 36.46, 35.31, 26.53; HRMS-ESI + (m/z): calcd for $C_{20}H_{22}N_2O_3$ [M + H]$^+$: 339.1709, found: 339.1715.

Open Access Article. Published on 07 August 2023. Downloaded on 7/22/2025 8:26:15 PM.
This article is licensed under a Creative Commons Attribution-NonCommercial 3.0 Unported Licence.

4.2 Molecular docking

The interaction of the designed analogues of erianin with PC was conducted using Discovery Studio 2019. The X-ray crystal structure of PC (PDB ID: 3GB3) was retrieved from the Protein Data Bank (https://www.rcsb.org). In addition, the binding site spheres of PC that were used as the input site sphere were 18.5898, −49.3392, 24.6895, 16.7; the number of hotspots was 100. The conformations of the ligands were allowed to generate tautomers and isomers. Libdock scores were used to evaluate the binding ability with the enzyme.

4.3 Bioactivity assay

Cell culture. Hepatocellular carcinoma cell line HCCLM3 (obtained from Procell) was cultured with DMEM (Hyclone, Utah) supplemented with 10% (v/v) FBS (Gibco, New York), 1% (v/v) penicillin/streptomycin (Beyotime, Shanghai). All cells were cultured in an incubator with 5% CO_2 at 37 °C.

Cell viability assay. Cells were incubated in a 96-well plate with density of 1.5×10^4 per well. Overnight all cells with a density of 80% were treated with 1% DMSO (negative control), and erianin (positive control) and different concentrations (50 nM L^{-1}, 200 nM L^{-1}) of compounds **1–47** (all compounds had HPLC purity above 95%) for 48 h. No FBS DMEM with 10% (v/v) CCK-8 (Selleck, Houston) was added to each well and incubated for 1 h at 37 °C. The absorbance was determined at 450 nm to calculate the cell viability (%).

PC activity assay. To examine the PC inhibition activity of the synthetic compounds, we used a PC Assay Kit and followed the manufacturer's instructions (Comin Biotechnology Co., Ltd, Suzhou, China). After extracting the mitochondrial proteins, we incubated them with synthetic compounds **1–4**, **6**, **34–36** and erianin (10 nM) for 24 h. The sample (10 μL), 10 μL of 100 mM triethanolamine buffer (pH 8.0, consisting of 30 mM ATP and 450 mM sodium bicarbonate), and 180 μL of the working solution (containing malate dehydrogenase, acetyl coenzyme, and NADH) were mixed in a 96-well plate, and subsequently analysed to determine the mitochondrial PC activity at 340 nm. The absorbance ($A1$ and $A2$) values were recorded at 2 min intervals, and the PC activity was calculated as follows: $6.43 \times (A1 - A2)$.

Author contributions

X. M., X. L., F. W. and G. Z. designed the research. H. S., J. Y., Z. Q. and G. L. synthesized the corresponding compounds. L. L., Q. D. and L. X. evaluated the biological activity. J. W. performed the computational studies. X. M., X. L. and H. S. co-wrote the paper. All the authors discussed the results and commented on the paper.

Conflicts of interest

The authors have no conflicts of interest.

Acknowledgements

We thank the NMPA Key Laboratory for Quality Monitoring and Evaluation of Traditional Chinese Medicine, Chinese Materia Medica (2023NMPA-CDDC04); the National Natural Science Foundation of China (22001246, T2192971, 21977092); the start-up grant from Chengdu Institute of Biology, Chinese Academy of Sciences; the Biological Resources Program (KFJ-BRP-008) from Chinese Academy of Sciences; and the Sichuan Science and Technology Program (2022ZYD0047, 2022YFS0001), for the financial support.

References

1 H. Sung, J. Ferlay, R. L. Siegel, M. Laversanne, I. Soerjomataram, A. Jemal and F. Bray, *CA-Cancer J. Clin.*, 2021, **71**, 209–249.
2 J. M. Llovet, J. Zucman-Rossi, E. Pikarsky, B. Sangro, M. Schwartz, M. Sherman and G. Gores, *Nat. Rev. Dis Primers*, 2016, **2**, 16018.
3 A. Villanueva, Y. Hoshida, C. Battiston, V. Tovar, D. Sia, C. Alsinet, H. Cornella, A. Liberzon, M. Kobayashi, H. Kumada, S. N. Thung, J. Bruix, P. Newell, C. April, J. B. Fan, S. Roayaie, V. Mazzaferro, M. E. Schwartz and J. M. Llovet, *Gastroenterology*, 2011, **140**, 1501–1512.
4 T. Li, J. Fan, L. X. Qin, J. Zhou, H. C. Sun, S. J. Qiu, Q. H. Ye, L. Wang and Z. Y. Tang, *Ann. Surg. Oncol.*, 2011, **18**, 1955–1963.
5 Y. Y. Shao, W. Y. Shau, S. Y. Chan, L. C. Lu, C. H. Hsu and A. L. Cheng, *Oncology*, 2015, **88**, 345–352.
6 J. Bruix and J. M. Llovet, *Hepatology*, 2002, **35**, 519–524.
7 J. M. Llovet and J. Bruix, *Hepatology*, 2008, **48**, 1312–1327.
8 (*a*) J. M. Llovet, S. Ricci, V. Mazzaferro, P. Hilgard, E. Gane, J. F. Blanc, A. C. de Oliveira, A. Santoro, J. L. Raoul, A. Forner, M. Schwartz, C. Porta, S. Zeuzem, L. Bolondi, T. F. Greten, P. R. Galle, J. F. Seitz, I. Borbath, D. Häussinger, T. Giannaris, M. Shan, M. Moscovici, D. Voliotis and J. Bruix, *N. Engl. J. Med.*, 2008, **359**, 378–390; (*b*) A. L. Cheng, Y. K. Kang, Z. Chen, C. J. Tsao, S. Qin, J. S. Kim, R. Luo, J. Feng, S. Ye, T. S. Yang, J. Xu, Y. Sun, H. Liang, J. Liu, J. Wang, W. Y. Tak, H. Pan, K. Burock, J. Zou, D. Voliotis and Z. Guan, *Lancet Oncol.*, 2009, **10**, 25–34; (*c*) M. Kudo, R. S. Finn, S. Qin, K. H. Han, K. Ikeda, F. Piscaglia, A. Baron, J. W. Park, G. Han, J. Jassem, J. F. Blanc, A. Vogel, D. Komov, T. R. J. Evans, C. Lopez, C. Dutcus, M. Guo, K. Saito, S. Kraljevic, T. Tamai, M. Ren and A. L. Cheng, *Lancet*, 2018, **391**, 1163–1173.
9 J. Chen, J. A. Gingold and X. Su, *Trends Mol. Med.*, 2019, **25**, 1010–1023.
10 J. M. Llovet, R. K. Kelley, A. Villanueva, A. G. Singal, E. Pikarsky, S. Roayaie, R. Lencioni, K. Koike, J. Zucman-Rossi and R. S. Finn, *Nat. Rev. Dis. Primers*, 2021, **7**, 6.
11 J. C. Wallace, Distribution and biological functions of pyruvate carboxylase in nature, *Pyruvate Carboxylase*, ed.

 This journal is © The Royal Society of Chemistry 2023

Open Access Article. Published on 07 August 2023. Downloaded on 7/22/2025 8:26:15 PM.
This article is licensed under a Creative Commons Attribution-NonCommercial 3.0 Unported Licence.

D. B. Keech and J. C. Wallace, CRC Press, Boca Raton, 1985, pp. 5–64.

12 (*a*) T. Cheng, J. Sudderth, C. Yang, A. R. Mullen, E. S. Jin, J. M. Matés and R. J. DeBerardinis, *Natl. Acad. Sci.*, 2011, **108**, 8674–8679; (*b*) C. T. Hensley and R. J. DeBerardinis, *J. Clin. Invest.*, 2015, **125**, 495–497; (*c*) S. Cardaci, L. Zheng, G. MacKay, N. J. F. van den Broek, E. D. Mackenzie, C. Nixon, D. Stevenson, S. Tumanov, V. Bulusu, J. J. Kamphorst, A. Vazquez, S. Fleming, F. Schiavi, G. Kalna, K. Blyth, D. Strathdee and E. Gottlieb, *Nat. Cell Biol.*, 2015, **17**, 1317–1326; (*d*) T. W. M. Fan, A. N. Lane, R. M. Higashi, M. A. Farag, H. Gao, M. Bousamra and D. M. Miller, *Mol. Cancer*, 2009, **8**, 41; (*e*) O. Warburg, *Science*, 1956, **123**, 309–314; (*f*) N. S. Forbes, A. L. Meadows, D. S. Clark and H. W. Blanch, *Metab. Eng.*, 2006, **8**, 639–652.

13 T. N. Zeczycki, M. S. Maurice and P. V. Attwood, *Open Enzyme Inhib. J.*, 2010, **3**, 8–26.

14 Q. Lin, Y. He, X. Wang, Y. Zhang, M. Hu, W. Guo, Y. He, T. Zhang, L. Lai, Z. Sun, Z. Yi, M. Liu and Y. Chen, *Adv. Sci.*, 2020, **7**, 1903483.

15 P. L. MaJumder and M. Joardar, *Indian J. Chem., Sect. B: Org. Chem. Incl. Med. Chem.*, 1984, **23**(11), 1040–1042.

16 (*a*) X. Zhang, Y. Wang, X. Li, A. Yang, Z. Li and D. Wang, *Aging*, 2019, **11**, 10284–10300; (*b*) X. Liu, S. Dong, M. Dong, Y. Li, Z. Sun, X. Zhang, Y. Wang, L. Teng and D. Wang, *Int. J. Pharm.*, 2021, **607**, 121034; (*c*) H. Dong, M. Wang, C. Chang, M. Sun, F. Yang, L. Li, M. Feng, L. Zhang, Q. Li, Y. Zhu, Y. Qiao, T. Xie and J. Chen, *Biochem. Pharmacol.*, 2020, **182**, 114266.

17 Y. Sheng, Y. Chen, Z. Zeng, W. Wu, J. Wang, Y. Ma, Y. Lin, J. Zhang, Y. Huang, W. Li, Q. Zhu, X. Wei, S. Li, W. Wisanwattana, F. Li, W. Liu, A. Suksamrarn, G. Zhang, W. Jiao and F. Wang, *J. Med. Chem.*, 2022, **65**, 460–484.

18 H. Zhou, B. Yang, M. Hong, R. Ma and L. Sheng, *Arzneim. Forsch.*, 2009, **59**, 141–145.

19 X. Yi and X. Lan, *Biomed. Chromatogr.*, 2020, **34**, e4826.

20 G. R. Pettit, B. Toki, D. L. Herald, P. Verdier-Pinard, M. R. Boyd, E. Hamel and R. K. Pettit, *J. Med. Chem.*, 1998, **41**, 1688–1695.

21 H. H. Ko, L. T. Tsao, K. L. Yu, C. T. Liu, J. P. Wang and C. N. Lin, *J. Med. Chem.*, 2003, **11**, 105–111.

22 M. Y. Song, Q. R. He, Y. L. Wang, H. R. Wang, T. C. Jiang, J. J. Tang and J. M. Gao, *Int. J. Mol. Sci.*, 2020, **21**, 1817.

23 M. Medarde, R. P. L. Clairac, A. C. Ramos, E. Caballero, J. L. López, D. G. Grávalos and A. S. Feliciano, *Bioorg. Med. Chem. Lett.*, 1995, **5**, 229–232.

24 R. Shirai, K. Tokuda, Y. Koiso and S. Iwasaki, *Bioorg. Med. Chem. Lett.*, 1994, **4**, 699–704.

25 A. Marset, D. Caprioglio, S. Torretta, G. Appendino and A. Minassi, *Tetrahedron Lett.*, 2016, **57**, 1540–1543.

26 Z. l. Ma, X. j. Yan, L. Zhao, J. j. Zhou, W. Pang, Z. p. Kai and F. h. Wu, *J. Agric. Food Chem.*, 2016, **64**, 746–751.

27 F. H. Wu, Z. L. Ma, Z. P. Kai, L. L. Huang, D. D. Li and J. W. Huang, CN107365248A, 2017, 11. 21.

28 A. B. S. Maya, C. Pérez-Melero, C. Mateo, D. Alonso, J. L. Fernández, C. Gajate, F. Mollinedo, R. Peláez, E. Caballero and M. Medarde, *J. Med. Chem.*, 2005, **48**, 556–568.

29 R. Martín, P. Prieto, J. R. Carrillo, A. M. Rodríguez, A. de Cozar, P. G. Boj, M. A. Díaz-García and M. G. Ramírez, *J. Mater. Chem. C*, 2019, **7**, 9996–10007.